Endosomal signaling of delta opioid receptors is an endogenous mechanism and therapeutic target for relief from inflammatory pain

Nestor N. Jimenez-Vargas[a], Jing Gong[b], Matthew J. Wisdom[c], Dane D. Jensen[c,d], Rocco Latorre[c], Alan Hegron[c], Shavonne Teng[c], Jesse J. DiCello[e], Pradeep Rajasekhar[e], Nicholas A. Veldhuis[e,f], Simona E. Carbone[e], Yang Yu[a], Cintya Lopez-Lopez[a], Josue Jaramillo-Polanco[a], Meritxell Canals[g], David E. Reed[a], Alan E. Lomax[a], Brian L. Schmidt[d], Kam W. Leong[b], Stephen J. Vanner[a], Michelle L. Halls[e,1], Nigel W. Bunnett[c,1], and Daniel P. Poole[e,f,1]

[a]Gastrointestinal Diseases Research Unit, Division of Gastroenterology, Queen's University, Kingston, ON, Canada K7L 2V7; [b]Department of Biomedical Engineering, Fu Foundation School of Engineering and Applied Science, Columbia University, New York, NY 10032; [c]Department of Molecular Pathobiology, New York University College of Dentistry, New York, NY 10010; [d]Bluestone Center for Clinical Research, New York University College of Dentistry, New York, NY 10010; [e]Drug Discovery Biology, Monash Institute of Pharmaceutical Sciences, Monash University, Parkville, VIC 3052, Australia; [f]Australian Research Council Centre of Excellence in Convergent Bio-Nano Science and Technology, Monash University, Parkville, VIC 3052, Australia; and [g]Centre for Membrane Proteins and Receptors and Division of Physiology, Pharmacology, and Neuroscience, School of Life Sciences, Queen's Medical Centre, University of Nottingham, NG7 2RD Nottingham, United Kingdom

Whether G protein-coupled receptors signal from endosomes to control important pathophysiological processes and are therapeutic targets is uncertain. We report that opioids from the inflamed colon activate δ-opioid receptors (DOPr) in endosomes of nociceptors. Biopsy samples of inflamed colonic mucosa from patients and mice with colitis released opioids that activated DOPr on nociceptors to cause a sustained decrease in excitability. DOPr agonists inhibited mechanically sensitive colonic nociceptors. DOPr endocytosis and endosomal signaling by protein kinase C (PKC) and extracellular signal-regulated kinase (ERK) pathways mediated the sustained inhibitory actions of endogenous opioids and DOPr agonists. DOPr agonists stimulated the recruitment of $G\alpha_{i/o}$ and β-arrestin1/2 to endosomes. Analysis of compartmentalized signaling revealed a requirement of DOPr endocytosis for activation of PKC at the plasma membrane and in the cytosol and ERK in the nucleus. We explored a nanoparticle delivery strategy to evaluate whether endosomal DOPr might be a therapeutic target for pain. The DOPr agonist DADLE was coupled to a liposome shell for targeting DOPr-positive nociceptors and incorporated into a mesoporous silica core for release in the acidic and reducing endosomal environment. Nanoparticles activated DOPr at the plasma membrane, were preferentially endocytosed by DOPr-expressing cells, and were delivered to DOPr-positive early endosomes. Nanoparticles caused a long-lasting activation of DOPr in endosomes, which provided sustained inhibition of nociceptor excitability and relief from inflammatory pain. Conversely, nanoparticles containing a DOPr antagonist abolished the sustained inhibitory effects of DADLE. Thus, DOPr in endosomes is an endogenous mechanism and a therapeutic target for relief from chronic inflammatory pain.

pain | inflammation | G protein-coupled receptors | signaling | nanomedicine

G protein-coupled receptors (GPCRs) control essential pathophysiological processes. One-third of Food and Drug Administration-approved drugs target GPCRs (1). GPCRs at the plasma membrane detect extracellular ligands and couple to heterotrimeric G proteins. Plasma membrane signaling is rapidly terminated. GPCR kinases phosphorylate activated GPCRs, which increases the affinity for β-arrestins (βARRs) (2). βARRs uncouple GPCRs from G proteins and desensitize signaling, and also couple GPCRs to the clathrin endocytic machinery (3). βARRs also recruit GPCRs, G proteins, and mitogen-activated protein kinases to endosomes (4, 5). Endosomes are an important site of continued GPCR signaling (6–8).

GPCRs control multiple steps of pain transmission (9). Endosomal signaling of protease-activated receptor-2 in primary sensory neurons and of neurokinin 1 receptor (NK_1R) and calcitonin-like receptor (CLR) in second-order neurons mediates neuronal excitation and pain transmission (10–13). The δ-, μ- and κ-opioid receptors (DOPr, MOPr, and KOPr) inhibit excitation of primary sensory, spinal, and supraspinal neurons and thereby induce analgesia (14). In patients with inflammatory bowel disease (IBD), infiltrating lymphocytes release opioids that activate opioid receptors on nociceptors to suppress excitability, providing an endogenous system of pain control (15–19). It is not known whether opioid receptors at the plasma

Significance

G protein-coupled receptors are considered to function principally at the cell surface. We present evidence that the δ-opioid receptor (DOPr) signals from endosomes to cause a sustained inhibition of pain. Opioids from the inflamed human and mouse colon, along with selective agonists that evoked DOPr internalization, inhibited the excitability of nociceptors by a mechanism requiring DOPr endocytosis. DOPr in endosomes generated a subset of signals in subcellular compartments that inhibited neuronal excitability. A DOPr agonist that was encapsulated into nanoparticles designed to selectively activate DOPr in endosomes of nociceptors caused a long-lasting inhibition of neuronal excitability and pain. Our results support the hypothesis that endosomal signaling of DOPr is an endogenous mechanism and therapeutic target for relief from inflammatory pain.

PHARMACOLOGY

membrane or in endosomes mediate this endogenous analgesic pathway and are the optimal target for treatment of inflammatory pain.

Here we investigated the hypothesis that opioids from the inflamed colon activate DOPr in endosomes of nociceptors to evoke signals that cause long-lasting inhibition of excitability and analgesia, and that DOPr in endosomes is a superior therapeutic target for inflammatory pain.

Results

DOPr Inhibits Inflammatory Pain. We investigated whether opioids from the inflamed colon activate opioid receptors on nociceptors and decrease excitability. Segments of colon from healthy control (HC) mice and from mice with colitis induced by chronic administration of dextran sulfate sodium (cDSS) were incubated in culture medium for 24 h to allow opioid release into the supernatant (16–18). Mouse dorsal root ganglia (DRG) neurons were exposed to HC or cDSS supernatant for 60 min and then washed (Fig. 1A).

To assess sustained changes in excitability, the rheobase (minimum input current required to fire an action potential) of small-diameter neurons was measured by patch-clamp recordings at 30 min after washing (T = 30 min) (11). The rheobase of neurons exposed to cDSS supernatant was $29 \pm 6\%$ higher than that of neurons exposed to HC supernatant ($P < 0.05$), consistent with decreased excitability (Fig. 1 A and B). To examine whether these findings translate to IBD, supernatants were obtained from colonic biopsy specimens from HC patients and patients with chronic ulcerative colitis (cUC). The rheobase of neurons exposed to cUC supernatant was $62 \pm 16\%$ higher than that of neurons exposed to

HC supernatant ($P < 0.01$) (Fig. 1 C and D). Preincubation of neurons with the DOPr antagonist SDM25N (100 nM, 60 min) abolished the sustained effects of cDSS supernatant on rheobase, whereas the MOPr antagonist CTOP (100 nM, 60 min) had no effect (Fig. 1 E and F). Neither SDM25N nor CTOP affected the rheobase of neurons exposed to mouse HC supernatant (Fig. 1F). Thus, opioids from the inflamed colon cause a DOPr-mediated inhibition of nociceptors.

Endosomal DOPr Inhibits Nociceptor Excitability. To determine whether DOPr undergoes clathrin- and dynamin-mediated endocytosis in nociceptors, we isolated DRG neurons from knockin mice expressing DOPr fused to enhanced green fluorescent protein (DOPr-eGFP) (20). In vehicle-treated neurons, DOPr-eGFP was detected at the plasma membrane and in vesicles of the soma and neurites (Fig. 2A). The DOPr agonist DADLE (1 μM, 30 min) induced depletion of DOPr-eGFP from the plasma membrane and redistribution to endosomes. Dyngo4a (Dy4; 30 μM), which inhibits dynamin (21), and PitStop2 (PS2; 15 μM), which inhibits clathrin-mediated endocytosis (22), prevented DADLE-evoked endocytosis of DOPr-eGFP, as confirmed by quantification of plasma membrane and cytosolic DOPr-eGFP (Fig. 2B).

To examine the contribution of DOPr endocytosis to the inhibitory effects of endogenous opioids, we pretreated neurons with Dy4 or PS2 and then challenged them with cDSS, cUC, or HC supernatant. Neurons were washed, and rheobase was measured after 30 min. Dy4 and PS2 prevented the sustained increase in rheobase of neurons exposed to cDSS and cUC supernatants (Fig. 2 C and D). Inactive forms of Dy4 and PS2 do not affect the rheobase of nociceptors (11).

We similarly examined the contribution of endocytosis to the effects of DOPr- and MOPr-selective agonists on neuronal excitability. We exposed nociceptors to DOPr-selective agonists, including DADLE and SNC80 (10 nM, 15 min), which evoke βARR recruitment and DOPr endocytosis, and a 10-fold higher concentration of ARM390 (100 nM, 15 min), a weakly internalizing agonist (23) (Fig. 2E). Neurons were washed, and rheobase was measured immediately (T = 0 min) or 30 min (T = 30 min) after washing. DADLE and SNC80 caused both immediate (T = 0 min) and sustained (T = 30 min) increases in rheobase (Fig. 2 E and F). ARM390 increased rheobase at T = 0 min but not at T = 30 min (Fig. 2G). PS2 abolished the effects of DADLE and SNC80, but not of ARM390. The MOPr agonist DAMGO caused an immediate increase in rheobase that was not sustained and was inhibited by PS2 (Fig. 2H).

GPCRs in endosomes can activate protein kinase C (PKC) and extracellular signal-regulated kinases (ERKs), which control nociceptor excitability (11). To examine the role of these kinases in the sustained inhibitory actions of DOPr, we preincubated neurons with GF109203X (1 μM, 30 min), which inhibits PKC (24), or with PD98059 (50 μM, 30 min), which inhibits MEK1 (25). GF109203X and PD98059 abolished the sustained increase in rheobase (T = 30 min) to DADLE (Fig. 2 I and J).

To compare the chronic actions of DOPr agonists, neurons were incubated overnight with DADLE (100 nM) or ARM390 (300 nM). Neurons were washed, and rheobase was measured (Fig. 2K). DADLE caused both immediate (T = 0 min) and sustained (T = 30 min) increases in rheobase. PS2 blocked both phases (Fig. 2K). ARM390 caused an immediate increase (T = 0 min), but not a sustained (T = 30 min) increase, in rheobase, which was unaffected by PS2 (Fig. 2L). Thus, opioids from the inflamed colon and agonists that evoke DOPr endocytosis cause a sustained decrease in excitability of nociceptors that requires PKC and ERK signaling.

Endosomal DOPr Inhibits Colonic Afferent Activity. To assess whether endosomal DOPr signaling in the peripheral projections of colonic nociceptors mediates the inhibitory actions of opioids, we made extracellular recordings from lumbar splanchnic nerves innervating isolated segments of mouse distal colon (11). Nociceptors were identified by probing the colon or mesentery with von Frey filaments (VFF). Basal responses (1 g VFF, 100%) of each unit to repeated
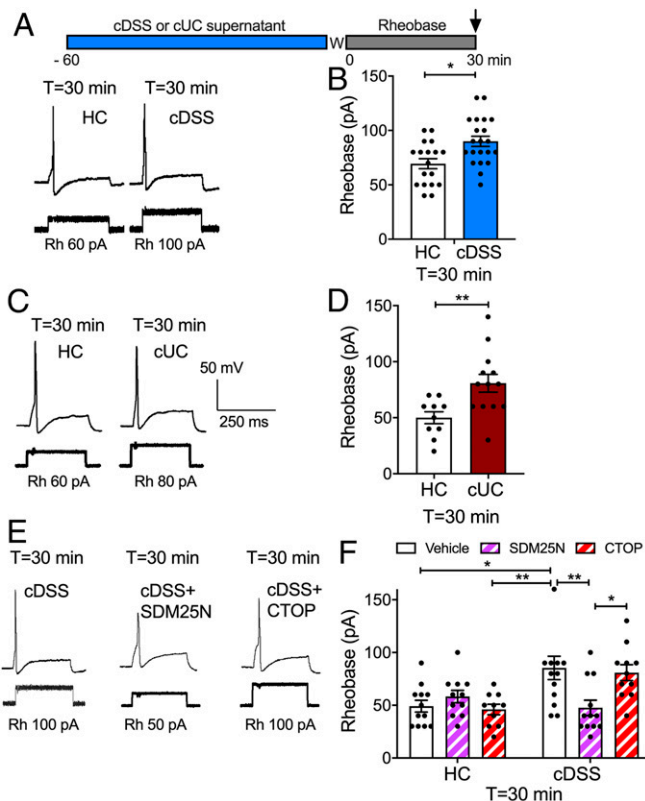
Fig. 1. Endogenous opioids and nociceptor excitability. Mouse DRG neurons were preincubated with supernatant from biopsies of HC, cDSS, or cUC colon and washed (W), and rheobase (Rh) was measured at 30 min after washing. Representative traces (A, C, and E) and pooled results (B, D, and F) of effects of supernatants from mouse (A, B, E, and F) and human (C and D) colonic biopsies. (E and F) Effects of antagonists of DOPr (SDM25N) or MOPr (CTOP) on responses to HC or cDSS supernatants. Data points indicate the number of studied neurons from n = 12 to 16 mice in B, 6 mice in D, and 8 mice in F for each treatment (mean ± SEM). *$P < 0.05$, **$P < 0.001$, two-way ANOVA with Tukey's post hoc test.
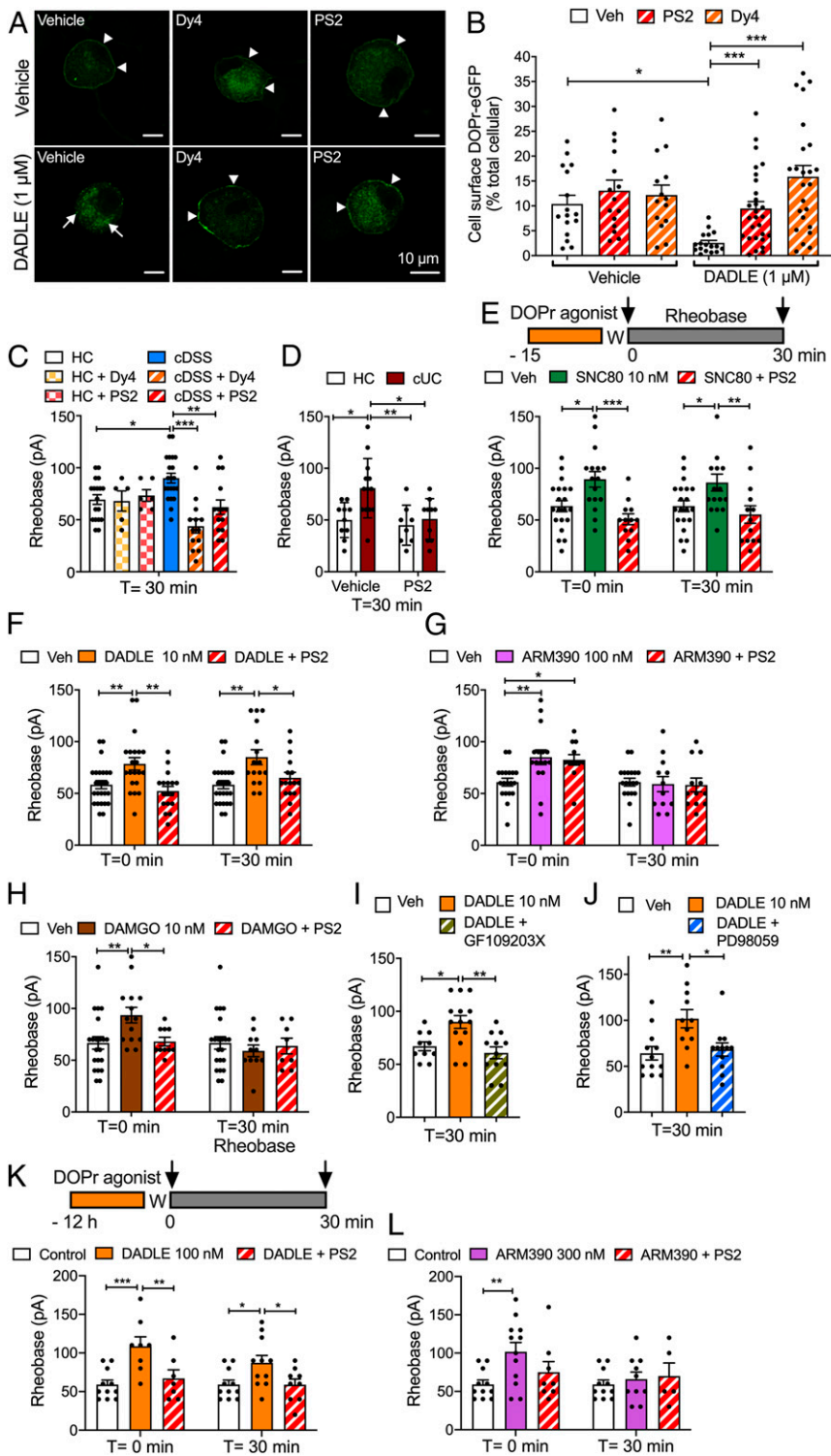
Fig. 2. Endosomal DOPr signaling and nociceptor excitability. (*A* and *B*) Endocytosis of DOPr-eGFP in DRG neurons from DOPr-eGFP mice. Neurons were incubated with vehicle (Veh) or DADLE (1 μM, 30 min), and DOPr-eGFP was localized by immunofluorescence. Neurons were preincubated with vehicle, Dy4, or PS2. (*A*) Representative images from four independent experiments. Arrowheads denote plasma membrane; arrows, endosomal DOPr-eGFP. (*B*) Quantification of the proportion of total cellular DOPr-eGFP at the plasma membrane. Data points indicate the number of studied neurons (N). *$P < 0.05$, ***$P < 0.001$, two-way ANOVA with Tukey's post hoc test. (*C–L*) Rheobase of mouse DRG neurons at 0 or 30 min after exposure to supernatant or DOPr agonists and washing. (*C* and *D*) Supernatant from cDSS, cUC, or HC biopsy specimens. (*E–J*) Neurons were incubated with the following agonists for 15 min and washed (W), and rheobase was measured at 0 or 30 min after washing: DOPr agonists SNC80 (*E*, 10 nM, internalizing), DADLE (*F*, 10 nM, internalizing) or ARM390 (*G*, 100 nM, weakly internalizing), and MOPr agonist DAMGO (*H*, 10 nM). In *C–H*, neurons were preincubated with Dy4, PS2, or vehicle. In *I* and *J*, neurons were preincubated with PKC inhibitor GF10923X or MEK1 inhibitor PD98059 before DADLE. (*K* and *L*) Neurons were incubated with the following agonists overnight and washed, and rheobase was measured at 0 or 30 min after washing: DADLE (*K*, 100 nM, internalizing) or ARM390 (*L*, 300 nM, weakly internalizing). Data points indicate the number of studied neurons from 12 to 16 mice in *C*, 6 mice in *D*, 10 to 15 mice in *E–J*, and 6 mice in *K* and *L* for each treatment (mean ± SEM). *$P < 0.05$, **$P < 0.01$, ***$P < 0.001$, one-way or two-way ANOVA with Tukey's post hoc test.

stimulation (three times for 3 s) were recorded (Fig. 3*A*). Agonists of DOPr (SNC80 and ARM390) or MOPr (DAMGO) (all 100 nM) were superfused into the organ bath for 15 min. Tissues were washed, and responses to VFF probing were reassessed every 15 min for 1 h. Compared with basal responses, DAMGO and ARM390 transiently inhibited the activity of colonic nociceptors, whereas SNC80 had a persistent inhibitory effect (Fig. 3 *B* and *C*). DAMGO maximally inhibited activity after 15 min of perfusion (i.e., 0 min,

53 ± 10% inhibition). ARM390 (weakly internalizing) inhibited activity only at 0 min (29 ± 4% inhibition). SNC80 (strongly internalizing) maximally inhibited activity at 30 min (33 ± 9% inhibition), which persisted for 60 min. PS2 (50 μM, 15 min) prevented the sustained inhibitory action of SNC80 (Fig. 3*D*). Thus, DOPr endosomal signaling within the peripheral projections of colonic nociceptors may induce a sustained inhibition of mechanical sensitivity.

PHARMACOLOGY
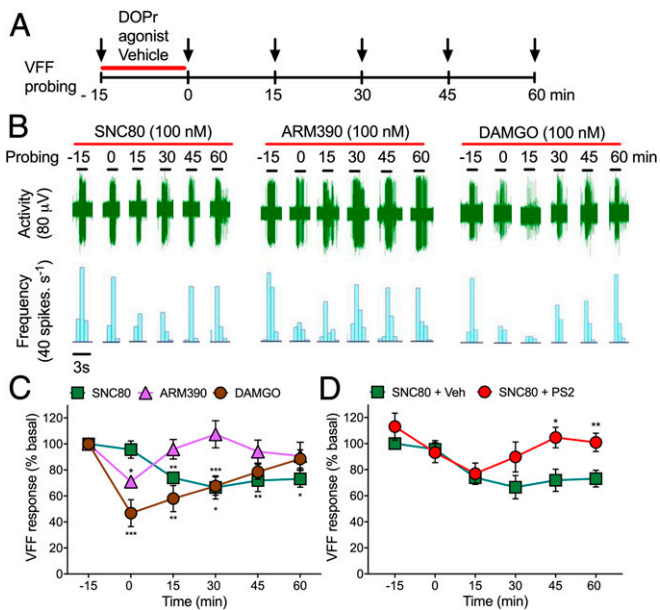
Fig. 3. MOPr and DOPr inhibition of colonic nociceptors. (*A*) Experimental protocol to examine MOPr and DOPr regulation of responses of colonic nociceptors to VFF probing. (*B*) Representative responses to agonists of DOPr (SNC80 and ARM390, 100 nM) and MOPr (DAMGO, 100 nM). (*C* and *D*) Time course of responses. In *D*, tissue was preincubated with PS2 or vehicle (Veh) before SNC80. $n = 5$ mice for each treatment. Data are mean ± SEM. *$P < 0.05$, **$P < 0.01$, ***$P < 0.001$, two-way ANOVA with Tukey's post hoc test.

DOPr Agonist Differentially Activate G Proteins, Recruit βARRs, and Stimulate Endocytosis.

We characterized the differential effects of DOPr agonists on receptor signaling and trafficking using bioluminescence resonance energy transfer (BRET) (26). HEK293 cells were transiently transfected with Gα-Rluc8 subtypes plus Gγ2-Venus, Gβ1, and DOPr. Gα-Rluc8/Gγ2-Venus BRET was measured to assess G protein dissociation (activation). SNC80, DADLE, and ARM390 (100 nM) decreased Gα$_{i1}$-Rluc8/Gγ2-Venus and Gα$_o$-Rluc8/Gγ2-Venus BRET, indicative of Gα$_{i/o}$ and Gβγ activation (*SI Appendix*, Fig. S1 *A* and *B*). SNC80, DADLE, and ARM390 had no effect on Gα$_s$-Rluc8/Gγ2-Venus BRET or Gα$_q$-Rluc8/Gα-Rluc8 BRET (*SI Appendix*, Fig. S1 *C* and *D*). SNC80, DADLE, and ARM390 decreased Gα$_{i1,2,3,o}$-Rluc8/Gγ2-Venus BRET with similar efficacy and an order of potency of DADLE > SNC80 > ARM390 (*SI Appendix*, Fig. S1 *E–G*).

To investigate βARR recruitment, HEK293 cells were transfected with DOPr-Rluc and βARR1/2-YFP. SNC80 and DADLE, but not ARM390 (all 100 nM), increased DOPr-Rluc/βARR1/2-YFP BRET (*SI Appendix*, Fig. S1 *H* and *I*). ARM390 increased BRET only at high concentrations (>1 μM). The order of potency for βARR recruitment was DADLE > SNC80 > ARM390 (*SI Appendix*, Fig. S1 *J* and *K*).

Thus, SNC80, DADLE, and ARM390 induce DOPr coupling to Gα$_{i/o}$, and SNC80 and DADLE, but not ARM390, stimulate DOPr coupling to βARR1/2. These results are consistent with the capacity of SNC80, but not of ARM390, to promote DOPr-eGFP phosphorylation, which is required for βARR recruitment (27).

To assess DOPr trafficking, we measured bystander BRET between DOPr-Rluc and Venus-tagged proteins resident of the plasma membrane (HRas-Venus, lipid rich; KRas-Venus, non–lipid-rich) and endosomes (Rab5a, early; Rab7a, late; Rab11a, recycling) (26). SNC80 and DADLE (100 nM) decreased BRET between DOPr-Rluc, HRas-Venus, and KRas-Venus (*SI Appendix*, Fig. S1 *L* and *M*). These changes were mirrored by an increase in BRET between DOPr-Rluc and Rab5a-Venus (*SI Appendix*, Fig. S1*N*). SNC80 stimulated BRET between DOPr-Rluc and Rab7a-Venus (*SI Appendix*, Fig. S1*O*). ARM390 (100 nM) did not affect BRET between

DOPr and plasma membrane or endosomal proteins. SNC80, DADLE, or ARM390 did not affect BRET between DOPr-Rluc and Rab11a-Venus (*SI Appendix*, Fig. S1*P*). Thus, SNC80 and DADLE cause DOPr internalization to early endosomes, whereas ARM390 does not. Internalized DOPr traffics to degradatory pathways in neurons (28).

DOPr Agonists Differentially Activate G Proteins and βARRs at the Plasma Membrane and in Endosomes.

To assess activation of G proteins at the plasma membrane and in endosomes of HEK293 cells, we measured enhanced bystander (eb) BRET between mini-G proteins (Rluc8-mGα$_{si/o/s/sq}$) (29, 30) and *Renilla* (R) GFP-CAAX (prenylation CAAX box of KRas) (31) for plasma membrane activation or tandem (td) RGFP-Rab5a for early endosome activation. Whereas Gα proteins associate with Gβγ subunits and GPCRs in the plasma membrane, mini-Gα proteins are N-terminally truncated and freely diffuse throughout the cytoplasm. Mini-Gα proteins can translocate to active GPCRs at the plasma membrane or in organelles. Mini-Gα$_{si}$ and Gα$_{sq}$ proteins were developed by mutating mGα$_s$ residues to equivalent Gα$_q$ and Gα$_i$ residues. Recruitment of βARRs was assessed by measuring ebBRET between Rluc8-βARR1 (32) or Rluc2-βARR2 (31) and RGFP-CAAX or tdRGFP-Rab5a. Rab5a was localized to endosomes (*SI Appendix*, Fig. S2*A*). SNC80, DADLE, and ARM390 (100 nM) increased Rluc8-mGα$_{si/o}$/RGFP-CAAX ebBRET (*SI Appendix*, Fig. S2 *B–E*) but did not affect Rluc8-mGα$_{s/sq}$/RGFP-CAAX ebBRET (*SI Appendix*, Fig. S2 *F* and *G*). SNC80 and DADLE, but not ARM390, increased Rluc8-βARR1 or Rluc2-βARR2/RGFP-CAAX ebBRET (*SI Appendix*, Fig. S2 *H–K*). SNC80 and DADLE, but not ARM390, increased Rluc8-mGα$_{si/o}$/tdRGFP-Rab5a ebBRET (*SI Appendix*, Fig. S2 *L–O*). These agonists did not affect Rluc8-mGα$_{s/sq}$/tdRGFP-Rab5a ebBRET (*SI Appendix*, Fig. S2 *P* and *Q*). SNC80 and DADLE, but not ARM390, increased Rluc8-βARR1 or Rluc2-βARR2/tdRGFP-Rab5a ebBRET (*SI Appendix*, Fig. S2 *R–U*). Pertussis toxin blunted βARR recruitment to the plasma membrane (*SI Appendix*, Fig. S2 *H–K*) and endosomes (*SI Appendix*, Fig. S2 *R–U*), indicating involvement of Gα$_{i/o}$ signaling.

The foregoing results suggest that SNC80, DADLE, and ARM390 activate Gα$_{i/o}$ at the plasma membrane. Only agonists that strongly internalize DOPr (SNC80 and DADLE) activate Gα$_{i/o}$ in endosomes and recruit βARR1/2 to the plasma membrane and endosomes.

Endosomal DOPr Activates a Subset of Compartmentalized Signals.

To examine DOPr signaling in subcellular compartments, we expressed DOPr and Förster resonance energy transfer (FRET) biosensors targeted to the plasma membrane, cytosol, or nucleus in HEK293 cells (10, 33). FRET biosensors included pmCKAR (plasma membrane PKC), cytoCKAR (cytosolic PKC), cytoEKAR (cytosolic ERK), and nucEKAR (nuclear ERK) (Fig. 4). To probe the link between endocytosis and compartmentalized signaling, we compared the effects of strongly internalizing (SNC80 and DADLE) and weakly internalizing (ARM390) DOPr agonists and used inhibitors of clathrin and dynamin.

SNC80 and DADLE (100 nM) stimulated a sustained increase in plasma membrane and cytosolic PKC activity (Fig. 4 *A–C*). ARM390 (100 nM) did not affect plasma membrane or cytosolic PKC activity. All three agonists stimulated a sustained increase in cytosolic ERK activity (Fig. 4 *D* and *F*). SNC80 and DADLE, but not ARM390, caused sustained activation of nuclear ERK (Fig. 4 *E* and *F*). These results suggest that DOPr signals from endosomes to activate plasma membrane and cytosolic PKC and nuclear ERK.

To assess the importance of endocytosis for compartmentalized signaling, we expressed wild-type (WT) dynamin or K44E dominant negative mutant dynamin (K44E dynamin) (34), or treated cells with PS2 or the inactive analog PS2 inactive. In control experiments with WT dynamin and PS2 inactive, SNC80 and DADLE induced rapid and sustained increases in PKC activity at the plasma membrane and in the cytosol (Fig. 5 *A–F*). Dynamin K44E and PS2 abolished SNC80 and DADLE stimulation of PKC at the plasma membrane and in the cytosol (Fig. 5 *A–F* and *SI Appendix*, Fig. S3 *A* and *B*). SNC80 and DADLE induced a gradual and sustained increase in
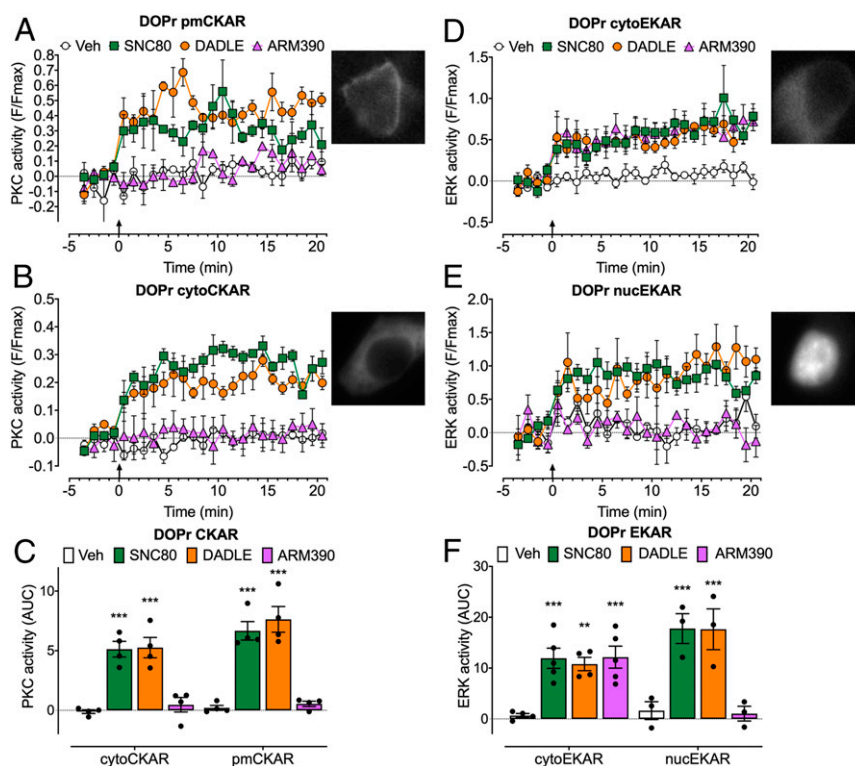
Fig. 4. DOPr-mediated PKC and ERK signaling in subcellular compartments of HEK293 cells. FRET biosensors for pmCKAR and cytoCKAR or cytoEKAR and nucEKAR were coexpressed with DOPr. *Insets* show cellular localization of FRET biosensors. Agonists (all 100 nM) or vehicle (Veh) were administered at the arrows. (*A* and *B*) Time course of plasma membrane (*A*) and cytosolic (*B*) PKC. (*C*) Integrated responses of plasma membrane and cytosolic PKC over 20 min (area under the curve [AUC]). (*D* and *E*) Time course of activation of cytosolic (*D*) and nuclear (*E*) ERK. (*F*) Integrated responses of cytosolic and nuclear ERK over 20 min (AUC). Data points show results of individual experiments. $n = 4$ (*A–C*), $n = 5$ cytoEKAR, $n = 3$ nucEKAR (*D–F*) independent experiments. Data are mean ± SEM. **$P < 0.01$, ***$P < 0.001$ ligand to vehicle, one-way ANOVA with Tukey's post hoc test.

ERK activity in the cytosol and nucleus (Fig. 5 *G–L*). Dynamin K44E and PS2 did not affect SNC80- and DADLE-induced cytosolic ERK activity but abolished SNC80- and DADLE-induced nuclear ERK activity (Fig. 5 *G–L* and *SI Appendix*, Fig. S3 *C* and *D*). The contribution of βARR1/2 to signaling was examined by siRNA knockdown (10, 26). βARR1/2 siRNA, but not scrambled siRNA (control), inhibited SNC80-induced activation of nuclear, but not cytosolic, ERK (Fig. 5 *M–O*).

To evaluate DOPr compartmentalized signaling in nociceptors, we expressed FRET biosensors in DRG neurons from DOPr-eGFP mice. SNC80 and DADLE stimulated sustained activation of PKC at the plasma membrane and in the cytosol (Fig. 6 *A–C*) and of ERK in the cytosol and nucleus (Fig. 6 *D–F*). ARM390 stimulated a sustained activation of cytosolic ERK but did not affect plasma membrane PKC or nuclear ERK activity. Dy4 abolished SNC80-stimulated activation of nuclear ERK, whereas cytosolic ERK activity was unaffected (Fig. 6 *G–J*). These results suggest that DOPr endocytosis in HEK293 cells and primary nociceptors mediates activation of plasma membrane and cytosolic PKC and nuclear ERK, but not of cytosolic ERK.

Nanoparticle-Encapsulated Agonists Target Endosomal DOPr. The realization that endosomal DOPr signaling mediates the inhibitory actions of opioids on nociceptor excitability suggests that agonists that activate DOPr in endosomes might provide effective relief from inflammatory pain. Nanoparticles can be used to deliver an NK$_1$R antagonist into endosomes of spinal neurons, where acidification triggers nanoparticle disassembly and antagonist release, leading to sustained antinociception (12). We incorporated DADLE into mesoporous silica nanoparticles (MSNs) designed to dissolve and release cargo in the acidic and reducing endosomal environment (35, 36) (Fig. 7*A*). For selective

targeting of DOPr-expressing neurons, we cloaked MSNs with PEGylated liposome covalently linked to DADLE.

Empty nanoparticles (LipoMSN), DADLE-coated nanoparticles (DADLE-LipoMSN), and nanoparticles with a DADLE coat and core (DADLE-LipoMSN-DADLE) were spherical with a hydrodynamic diameter of 140 to 210 nM, a surface charge of +28 to 36 mV, and a polydispersity index of 0.24 to 0.27 (Fig. 7 *B* and *C*). The loading efficiency of DADLE into the MSN core was 57 ± 6%. To examine MSN disassembly and cargo release, MSNs loaded with DADLE-Alexa647 (MSN-DADLE-Alexa647) were incubated in buffers at pH 7.2 or 5.2 or with or without 10 mM glutathione to mimic the acidic and reducing conditions of endosomes. The release of DADLE-Alexa647 into buffer was faster and more complete at pH 5.2 and in the presence of glutathione, and it continued for 24 h (Fig. 7 *D* and *E*).

To determine whether a DADLE-Lipo shell could facilitate selective uptake by DOPr-expressing cells, MSNs loaded with Alexa Fluor 647 and coated with DADLE-Lipo were incubated with untransfected HEK293 cells or HEK-DOPr cells for 2 h. The number of cells containing Alexa647 was determined by flow cytometry. DADLE-LipoMSN-Alexa647 was internalized into 66 ± 7% of HEK-DOPr cells, compared with 22 ± 1% of untransfected HEK293 cells ($P < 0.05$, t test), indicating preferential delivery to cells expressing DOPr (Fig. 7*F*). Dy4 and PS2, but not inactive analogs, inhibited DADLE-LipoMSN-Alexa647 uptake by HEK-DOPr cells, consistent with clathrin- and dynamin-mediated endocytosis (Fig. 7*G*).

To determine whether nanoparticles target DOPr in endosomes, HEK-HA-DOPr cells expressing Rab5a-GFP were incubated with HA antibodies to label surface DOPr. Cells were incubated with DADLE-LipoMSN-Alexa647 (20 μM DADLE, 200 μg/mL LipoMSN) and imaged by confocal microscopy. DADLE-LipoMSN-Alexa647 accumulated at the plasma membrane, stimulated endocytosis of HA-DOPr, and colocalized with HA-DOPr in early endosomes at 30 min (Fig. 7*H* and
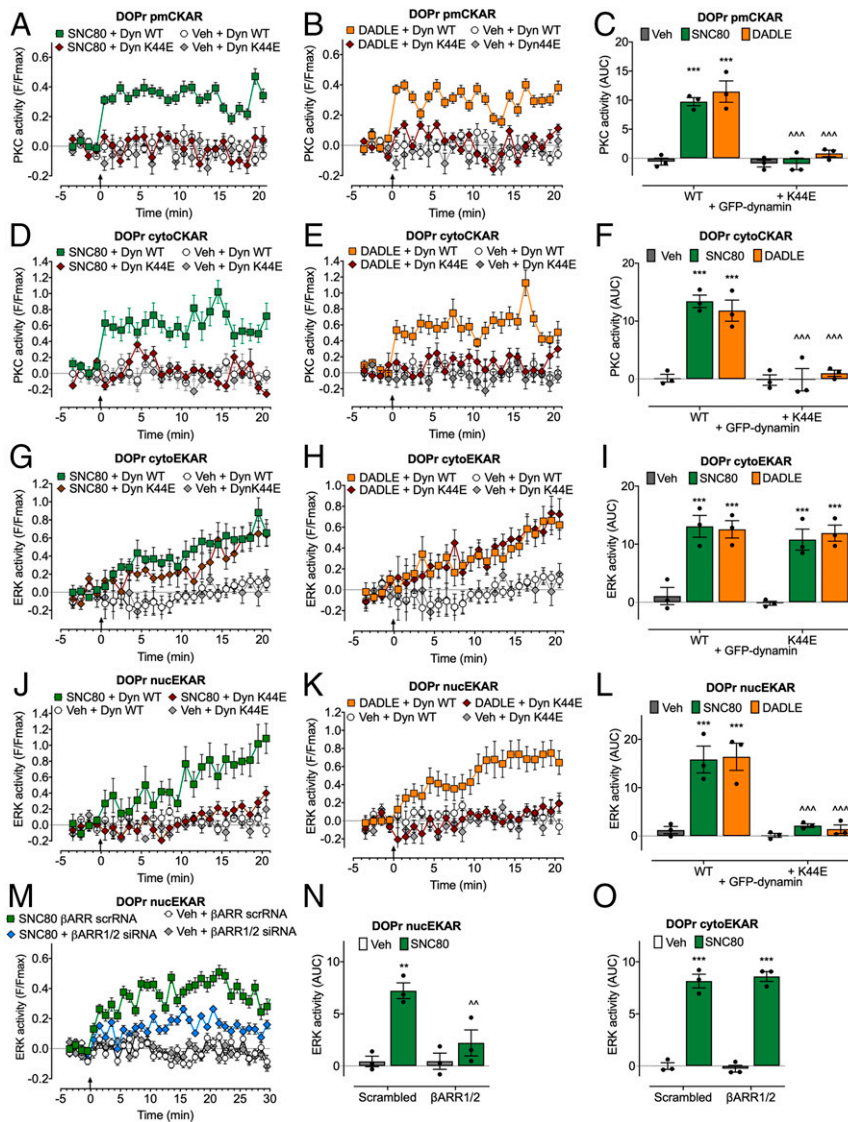
Fig. 5. Endosomal DOPr-mediated PKC and ERK signaling in subcellular compartments of HEK293 cells. FRET biosensors for pmCKAR and cytoCKAR or cytoEKAR and nucEKAR were coexpressed with DOPr and either dynamin WT (Dyn WT) or dominant negative dynamin K44E (Dyn K44E) (*A–L*) or with βARR1+2 siRNA or scrambled (scr) siRNA (control) (*M–O*). Agonists (all 100 nM) or vehicle (Veh) were administered at the arrows. (*A–C*) Plasma membrane PKC activity. (*D–F*) Cytosolic PKC activity. (*G–I* and *O*) Cytosolic ERK activity. (*J–N*) Nuclear ERK activity. (*A, B, D, E, G, H, J, K,* and *M*) Time course of responses. (*C, F, I, L, N,* and *O*) Integrated responses over 20 or 30 min (AUC). Data points show results of individual experiments. $n = 3$ independent experiments. Data are mean ± SEM. **$P < 0.01$, ***$P < 0.001$ ligand to vehicle; ^^$P < 0.01$, ^^^$P < 0.001$ inhibitors to control; two-way ANOVA with Tukey's post hoc test.

SI Appendix, Fig. S4*A*). Live cell imaging, which avoided the loss of nanoparticle fluorescence during immunostaining, revealed DADLE-LipoMSN-Alexa647 binding to the plasma membrane and uptake into Rab5a-GFP endosomes within 30 min (Movie S1). Control LipoMSN-Alexa647, lacking the DADLE targeting group, showed diminished uptake (Movie S2).

We examined whether DADLE nanoparticles activate DOPr signaling at the plasma membrane (inhibition of cAMP, βARR1 recruitment) and in endosomes (nuclear ERK). Compared with Lipo-MSN or vehicle, DADLE (100 nM), DADLE-LipoMSN (20 μM DADLE), and DADLE-LipoMSN-DADLE (20 μM DADLE) inhibited forskolin (10 μM)-stimulated formation of cAMP in HEK-DOPr cells but not in untransfected HEK293 cells (Fig. 7*I* and *SI Appendix*, Fig. S4 *B* and *C*). DADLE and DADLE-LipoMSN-DADLE increased DOPr-Rluc8/βARR1-YFP BRET (Fig. 7*J* and *SI Appendix*, Fig. S4*D*). DADLE, DADLE-LipoMSN, and DADLE-LipoMSN-DADLE activated nuclear ERK, which was particularly sustained for DADLE-LipoMSN and DADLE-LipoMSN-DADLE (Fig. 7*K* and *SI Appendix*, Fig. S4*E*). These results suggest that DADLE coupled to the liposome shell

can activate DOPr at the plasma membrane and stimulate DOPr endocytosis. DADLE released from the MSN core in endosomes might activate DOPr to stimulate nuclear ERK activity.

Primary cultures of DRG neurons from DOPr-eGFP knockin mice were studied to assess nanoparticle targeting and uptake into neurons. Neurons were incubated with DADLE, LipoMSN-Alexa647 (control), or DADLE-LipoMSN-Alexa647 (1 μM, 60 min, 37 °C) and fixed. GFP and the neuronal marker Hu were localized by immunofluorescence. DADLE evoked endocytosis of DOPr-eGFP in neurons (*SI Appendix*, Fig. S5*A*). LipoMSN-Alexa647 was detected at the surface of some neurons but did not promote DOPr-eGFP endocytosis (Fig. 8*A*). DADLE-LipoMSN-Alexa647 evoked DOPr-eGFP internalization and colocalized in endosomes with DOPr-eGFP.

A Nanoparticle-Encapsulated DOPr Agonist Provides Long-Lasting Antinociception. To assess antinociception, DRG neurons were incubated with DADLE, DADLE-LipoMSN, or DADLE-LipoMSN-DADLE (100 nM DADLE) for 30 min and washed, and then rheobase was
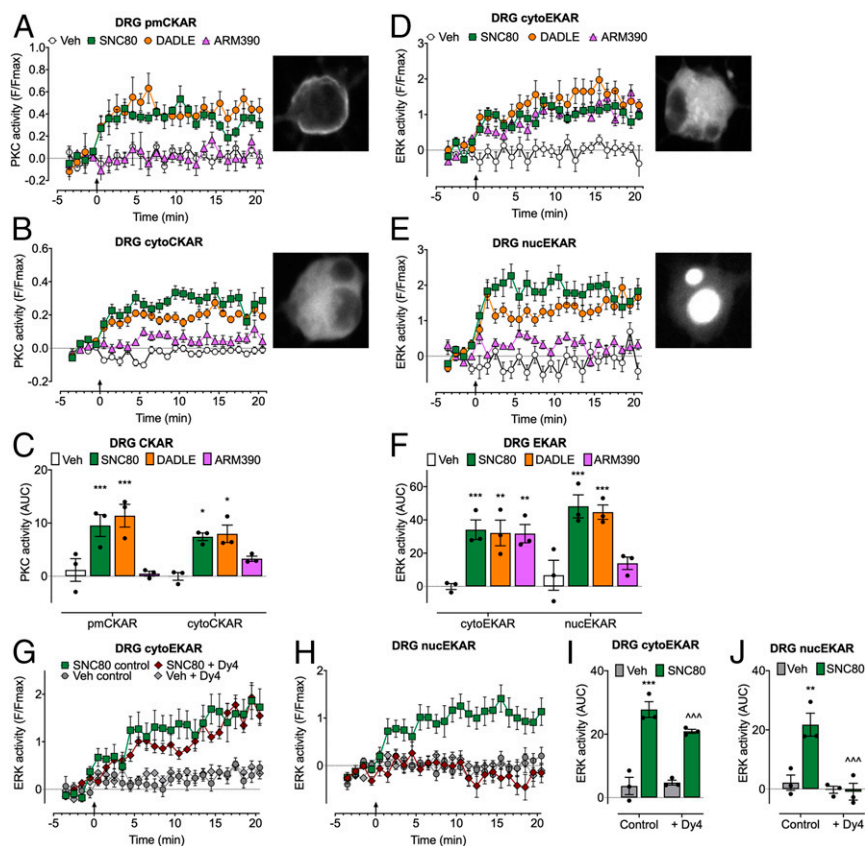
Fig. 6. Endosomal DOPr-mediated PKC and ERK signaling in subcellular compartments of DRG neurons. FRET biosensors for pmCKAR and cytoCKAR or cytoEKAR and nucEKAR were expressed in DRG neurons from DOPr-eGFP mice. *Insets* show localization of FRET biosensors. Agonists (all 100 nM) or vehicle (Veh) were administered at arrow. (*A* and *B*) Time course of plasma membrane (*A*) and cytosolic (*B*) PKC. (*C*) Effects of agonist treatments on PKC over 20 min (AUC). (*D* and *E*) Time course of cytosolic ERK (*D*) and nuclear ERK (*E*). (*F*) Effects of agonists on ERK activity over 20 min (AUC). (*G* and *H*) Time course of effects of dynamin inhibitor (Dy4) on cytosolic (*G*) and nuclear (*H*) ERK activity. (*I* and *J*) Effects of Dy4 treatments on ERK over 20 min (AUC). Data points show results of individual experiments. $n = 3$ independent experiments. Data are mean $\pm$ SEM. $*P < 0.05$, $**P < 0.01$, $***P < 0.001$ ligand to vehicle; $\wedge\wedge\wedge P < 0.001$ inhibitor to control; one-way ANOVA with Tukey's post hoc test.

measured at 0, 90, 120, or 180 min after washing. DADLE and DADLE-LipoMSN increased rheobase only at 0 min (Fig. 8 *B* and *C*). DADLE-LipoMSN-DADLE increased rheobase at 0, 90, and 120 min (26 ± 6% at 120 min). PS2 prevented the sustained inhibitory actions of DADLE-LipoMSN-DADLE (Fig. 8 *B* and *C*).

To assess the activity of peripheral colonic nociceptors, extracellular recordings were made from colonic afferents. DADLE-LipoMSN-DADLE (100 nM DADLE) was superfused into the organ bath for 30 min. Responses to VFF probing were assessed at 60 min and 120 min after washing. DADLE-LipoMSN-DADLE inhibited the activity of colonic nociceptors for at least 120 min (54 ± 13% inhibition) (Fig. 8*D*). PS2 prevented the sustained inhibitory action of DADLE-LipoMSN-DADLE.

To assess inflammatory nociception, complete Freund's adjuvant (CFA) was administered to mice by intraplantar injection, and withdrawal responses to stimulation of the plantar surface of the ipsilateral paw with VFFs were measured after 48 h. When administered by intrathecal injection to target DOPr on the central projections of nociceptors and on spinal neurons, DADLE (100 nM, 5 µL) had a moderate and transient antinociceptive action, whereas DADLE-LipoMSN-DADLE (100 nM DADLE, 5 µL) had a strong antinociceptive action that was sustained for 6 h (Fig. 8*E*). LipoMSN (1 µg/mL, 5 µL) had no effect. Nanoparticles did not affect withdrawal responses of the contralateral paw (*SI Appendix*, Fig. S5*B*). Thus, neuronal-targeted stimulus-responsive nanoparticles provide long-lasting antinociception.

A Nanoparticle-Encapsulated DOPr Antagonist Prevents the Sustained Antinociceptive Actions of DOPr. To provide evidence that DOPr endosomal signaling underlies sustained inhibition of neuronal

excitability, we encapsulated the DOPr antagonist SDM25N into nanoparticles with a liposome shell (LipoMSN-SDM25N). LipoMSN-SDM25N had a hydrodynamic diameter of 176.5 ± 0.6 nm, a surface charge of +32 ± 3 mV, and a polydispersity index of 0.15 ± 0.02. SDM25N loading efficiency was 73.5 ± 0.8%. To assess the uptake of nanoparticles lacking the DADLE targeting group, LipoMSN-Alexa647 nanoparticles were incubated with HEK293 cells (0 to 4 h, 37 °C). After 120 min, LipoMSN-Alexa647 was detected in Rab5a-positive early endosomes (Fig. 8*F*). LipoMSN-Alexa647 was internalized in 67.7 ± 1.3% of HEK293 cells after 120 min, as assessed by flow cytometry (Fig. 8*G*). To determine whether an endosomally targeted DOPr antagonist can block nociception, DRG neurons were incubated with LipoMSN-SDM25N (100 nM SDM25N, 100 µg/mL LipoMSN) or LipoMSN (100 µg/mL, control) (120 min, 37 °C) (Fig. 8*H*), then washed, incubated with DADLE (10 nM, 15 min) and washed again. Rheobase was measured at 0 and 30 min after washing. In LipoMSN-treated neurons, DADLE increased rheobase at 0 min (53.44 ± 17.1%) and 30 min (55.56 ± 10.07%) compared with control. LipoMSN-SDM25N had no effect on the rheobase at 0 min (52.18 ± 13.78%) but abolished the inhibitory effect of DADLE at 30 min. These results support the hypothesis that DOPr signals from endosomes to cause persistent antinociception.

Discussion

Our results support the hypothesis that DOPr in endosomes is as a key component of an endogenous mechanism of pain control, and

that endosomal DOPr is a viable therapeutic target for chronic inflammatory pain.

Antinociceptive Signaling of Endosomal DOPr. Several observations suggest that DOPr signaling in endosomes mediates the sustained antinociceptive actions of endogenous opioids and certain DOPr-selective agonists (*SI Appendix*, Fig. S6). Biopsy specimens of inflamed human and mouse colon released opioids that caused a sustained inhibition of the excitability of nociceptors, as revealed by increased rheobase. These effects are attributable to DOPr, because a selective antagonist prevented inhibition. Colitis evokes endocytosis of DOPr-eGFP in myenteric neurons, consistent with opioid release and DOPr activation (37). Our findings support reports of an opioid-mediated mechanism of antinociception in inflamed colon (15–19). DOPr agonists that stimulated robust receptor endocytosis (DADLE and SNC80) caused a persistent inhibition of nociceptor excitability, whereas a weakly internalizing DOPr agonist (ARM390) had only a transient inhibitory action. Inhibitors of clathrin and dynamin prevented agonist-evoked endocytosis of DOPr-eGFP in nociceptors and blocked the sustained inhibitory actions of endogenous opioids and internalizing DOPr agonists.

These results support a role for endosomal signaling of DOPr in regulating sustained excitability of the soma, which was examined by patch clamp recordings. Similar mechanisms may control the excitability of nerve endings in the colon, since SNC80 caused a long-lasting inhibition of mechanically sensitive nociceptors, whereas weakly internalizing ARM390 did not. A clathrin inhibitor blocked the effects of SNC80, which require endosomal signaling. DOPr endocytosis has also been linked to analgesic tolerance (23, 27, 38, 39). A DOPr antagonist (SDM25N) incorporated into nanoparticles designed to deliver and release cargo in endosomes prevented the sustained inhibitory actions of DADLE on nociceptor excitability. These findings suggest that DADLE continues to activate DOPr in endosomes to inhibit nociception.

Our results do not exclude a role for plasma membrane signaling of DOPr in antinociception. Inhibitors of endocytosis and nanoparticle-encapsulated SDM25N did not affect the short-term inhibitory effects of DOPr agonists on excitability. Thus, DOPr signaling at the plasma membrane and in endosomes mediates antinociception, but with different time courses.

Our results reveal spatial and temporal differences in the way in which DOPr and MOPr regulate the excitability of nociceptors. A MOPr antagonist did not prevent the inhibitory actions of colonic supernatants on neuronal excitability, suggesting that MOPr does not contribute antinociception during colitis. Although the MOPr agonist DAMGO transiently decreased the excitability of DRG neurons and colonic afferents, these effects were not sustained. A clathrin inhibitor prevented the transient inhibitory actions of DAMGO, which likely require endosomal signaling of MOPr. These results are in agreement with studies in which a conformationally selective nanobody was used to detect activated MOPr in subcellular compartments (40).

Biophysical approaches were used to examine DOPr trafficking and signaling in HEK-DOPr cells and nociceptors, with consistent results. All DOPr agonists (DADLE, SNC80, and ARM390) activated $G\alpha_{i/o}$ with similar efficacy. Only strongly internalizing agonists (DADLE and SNC80) potently recruited βARR1/2 and stimulated DOPr depletion from the plasma membrane and accumulation and retention in early endosomes. The results confirm reported differences in the ability of DADLE, SNC80, and ARM390 to promote DOPr internalization (23). These differences are attributable to GRK-induced DOPr phosphorylation; SNC80 induces DOPr phosphorylation at Ser[363], whereas ARM390 does not (27).

The use of FRET biosensors targeted to the plasma membrane, cytosol, or nucleus revealed that DOPr endocytosis is necessary for a subset of signals in subcellular compartments. Our results suggest that DOPr signaling from the plasma membrane activates ERK in the cytosol, whereas DOPr signaling in endosomes activates PKC at the plasma membrane and in the cytosol and activates ERK in the nucleus but not in the cytosol. Support for these conclusions derives from the observation that internalizing agonists alone activated plasma membrane and cytosolic PKC and nuclear ERK. Inhibitors of clathrin- and dynamin-mediated endocytosis, dominant negative dynamin, and βARR1/2 knockdown selectively suppressed these signals. Other GPCRs also signal from endosomes to regulate subsets of compartmentalized signals (10, 11, 13). Inhibitors of PKC and MEK1 prevented the sustained inhibitory actions of DADLE on neuronal excitability, providing a link between endosomal DOPr signaling and antinociception. PKC is a critical regulator of DOPr-mediated signaling and antinociception (41). DOPr endocytosis is also required for ERK activation and trafficking to perinuclear and nuclear locations (42).

$G\alpha_{i/o}$ and βARRs may mediate endosomal DOPr signaling, since internalizing, but not weakly internalizing, DOPr agonists stimulated the recruitment of mini-$G\alpha_{i/o}$ and βARR1/2 to early endosomes, as determined by BRET. βARR1/2 knockdown inhibited SNC80-stimulated nuclear ERK activation, possibly due to inhibition of DOPr endocytosis and endosomal signaling. Further studies are needed to determine the contribution of βARRs and $G\alpha_{i/o}$ to endosomal DOPr signaling.

Therapeutic Targeting of Endosomal DOPr. The realization that GPCRs can signal from endosomes to mediate pain has revealed endosomal GPCRs as a viable therapeutic target (8). Conjugation to transmembrane lipids or encapsulation into pH-tunable nanoparticles delivers antagonists of pronociceptive GPCRs to endosomes (10–13). Endosomally targeted antagonists preferentially inhibit endosomal signaling and provide enhanced antinociception compared with conventional antagonists. The present study shows that endosomally targeted agonists of antinociceptive GPCRs also provide long-lasting pain relief. DADLE-LipoMSN-DADLE inhibited nociceptor excitability for at least 3 h after washout, in contrast to the transient inhibitory action of free DADLE. DADLE-LipoMSN-DADLE caused a long-lasting inhibition of mechanically evoked activation of colonic nociceptors and effectively reversed inflammatory nociception. One component of the enhanced antinociceptive properties of nanoparticles might relate to the selective delivery of primary sensory neurons to endosomes. Targeted delivery to DOPr-expressing neurons was accomplished by cloaking MSNs with PEGylated liposomes covalently linked to DADLE. DADLE-LipoMSNs retained the ability to activate DOPr in HEK-DOPr cells, as assessed by inhibition of cAMP, recruitment of βARR1, stimulation of DOPr endocytosis, and activation of nuclear ERK (*SI Appendix*, Fig. S6). Uptake of DADLE-LipoMSNs by HEK-DOPr cells was threefold greater than that by untransfected HEK cells, suggesting preferential targeting. DADLE-LipoMSNs entered cells by clathrin-mediated endocytosis and were delivered to DOPr-positive early endosomes. Another component of enhanced antinociception could be the sustained activation of DOPr in endosomes, which was attained by incorporating DADLE into the MSN core. DADLE release was accelerated in the acidic and reducing endosomal environment and continued for 24 h. The finding that a clathrin inhibitor abrogated the antinociceptive actions of DADLE-LipoMSN-DADLE indicates a requirement for nanoparticle endocytosis.

More direct evidence for a role of endosomal DOPr in antinociception was provided by incorporating the DOPr antagonist SDM25N into nanoparticles. When preincubated with neurons to allow for endosomal accumulation, followed by extensive washing to remove extracellular antagonist, LipoMSN-SDM25N prevented the sustained inhibitory actions of DADLE on nociceptor excitability, supporting endosomal signaling. The immediate inhibitory actions of DADLE were unaffected and likely arose from plasma membrane DOPr.

Incorporation into nanoparticles can enhance the stability and delivery of drugs, thereby improving efficacy (43–45). Stimulus-responsive nanoparticles deliver combinations of chemotherapeutics to tumors, where increased vascular permeability and extracellular acidification promote delivery and cargo release (46, 47). Although nanoparticles are often endocytosed, endosomal disruption is necessary for drug delivery to cytosolic and nuclear targets, which can compromise efficacy (48). The discovery of GPCRs in endosomes as therapeutic targets provides an opportunity to use nanoparticles to deliver treatments for pain (8). Our results
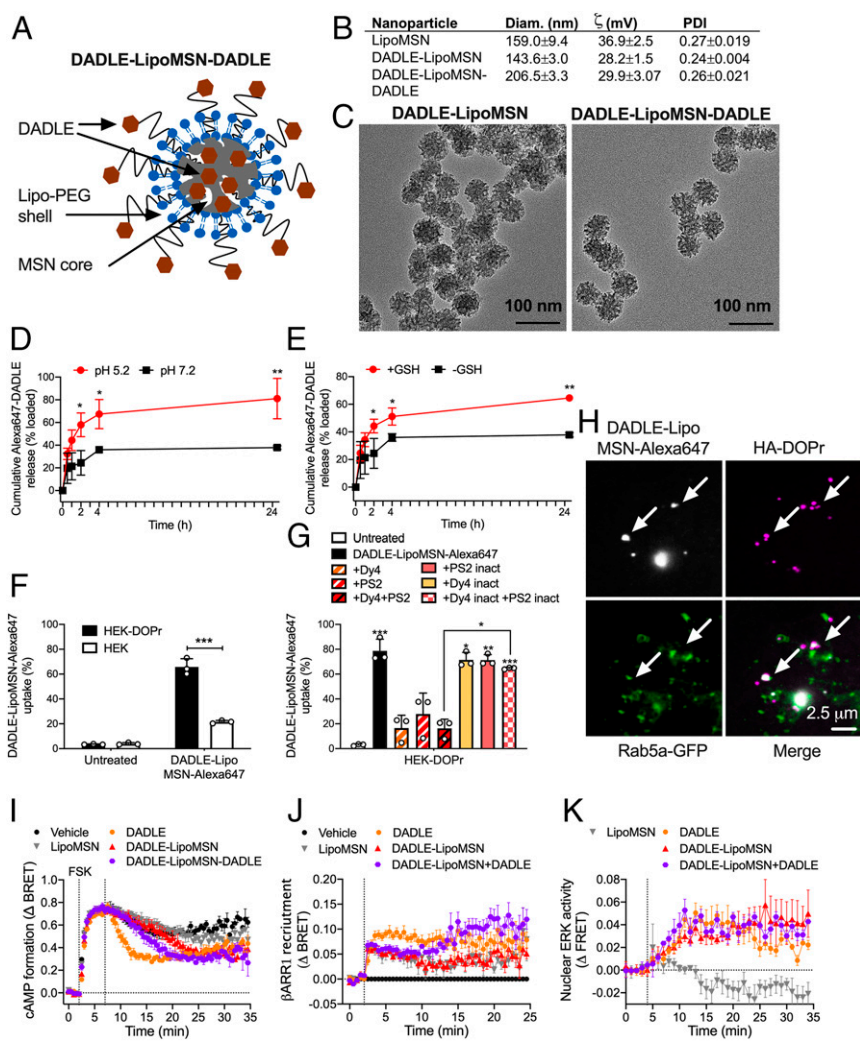
Fig. 7. Characterization of nanoparticles. (*A*) Structure of DADLE-LipoMSN-DADLE. (*B*) Physical properties of nanoparticles. $n = 4$ experiments. (*C*) Transmission electron micrographs of DADLE-LipoMSN and DADLE-LipoMSN-DADLE. Representative images, $n = 3$ independent experiments. (*D* and *E*) Time course of in vitro release of DADLE-Alexa647 from MSN-DADLE-Alexa647 at graded pH (*D*) and glutathione concentrations (*E*). $n = 3$ independent experiments. *$P < 0.05$, **$P < 0.01$, t test with Holm–Sidak correction. (*F* and *G*) Uptake of DADLE-LipoMSN-DADLE-Alexa647 into HEK293 control and HEK-DOPr cells determined by flow cytometry. (*F*) Uptake into HEK293 control and HEK-DOPr cells after 2 h. ***$P < 0.001$, t test with Holm–Sidak correction. (*G*) Effects of inhibitors of clathrin and dynamin and inactive analogs on uptake into HEK-DOPr cells after 2 h. $n = 3$ independent experiments. *$P < 0.05$, **$P < 0.01$, ***$P < 0.001$ compared with untreated cells, one-way ANOVA with Tukey's post hoc test. (*H*) Uptake of DADLE-LipoMSN-DADLE-Alexa647 into HEK-HA-DOPr cells after 30 min. Arrows show colocalization of DADLE-LipoMSN-DADLE-Alexa647 with DOPr in Rab5a-positive early endosomes. Representative images from four independent experiments. (*I–K*) Effects of DADLE (100 nM), DADLE-LipoMSN (20 μM), and DADLE-LipoMSN-DADLE (20 μM) on forskolin (FSK; 10 μM)-stimulated cAMP formation (*I*), βARR1 recruitment (*J*), and activation of nuclear ERK (*K*). $n = 5$ independent experiments. All results are mean ± SEM.

demonstrate the feasibility of using nanoparticles to target nociceptors with consequent reductions in dose. Nanoparticles might allow the simultaneous delivery to endosomes of agonists or antagonists of several endosomal GPCRs involved in pain. Since multiple GPCRs control pain transmission (9), the ability to target multiple receptors in pain-transmitting neurons for prolonged periods might provide effective and long-lasting antinociception.

Nanoparticle-encapsulated GPCR ligands may have utility beyond the treatment of pain. GPCRs control many pathophysiological processes and are the targets of more than one-third of Food and Drug Administration-approved drugs (1). Many GPCRs internalize when activated and likely continue to signal from endosomes. The use of stimulus-responsive nanoparticles for delivery of drugs to endosomes of targeted cells might enhance efficacy with reduced doses and fewer side effects.

Limitations. This study has several limitations. We cannot exclude a possible role for plasma membrane signaling even in the sustained

inhibitory actions of opioids. The relative contributions of plasma membrane and endosomal signaling likely depend on the nature and concentration of the ligand and the time at which nociception is assessed. The differential effects of DOPr agonists that strongly (SNC80 and DADLE) or weakly (ARM390) promote endocytosis support a role for endosomal DOPr signaling for sustained antinociception. ARM390 is a partial agonist for βARR recruitment, which may explain its inability to cause long-lasting antinociception. We were unable to determine whether DOPr endosomal signaling involves G proteins and βARRs, which mediate endosomal signaling of other GPCRs (4, 5, 10, 11, 49, 50). Although dynamin and clathrin inhibitors blocked a subset of DOPr signals and inhibited sustained antinociception, these inhibitors also have nonspecific actions (51). Dominant negative dynamin and βARR knockdown replicated some effects of endocytosis inhibitors but could affect other functions as well. We cannot exclude the possibility that DOPr signals from intracellular compartments other than endosomes, since MOPr can signal from different compartments depending on the membrane
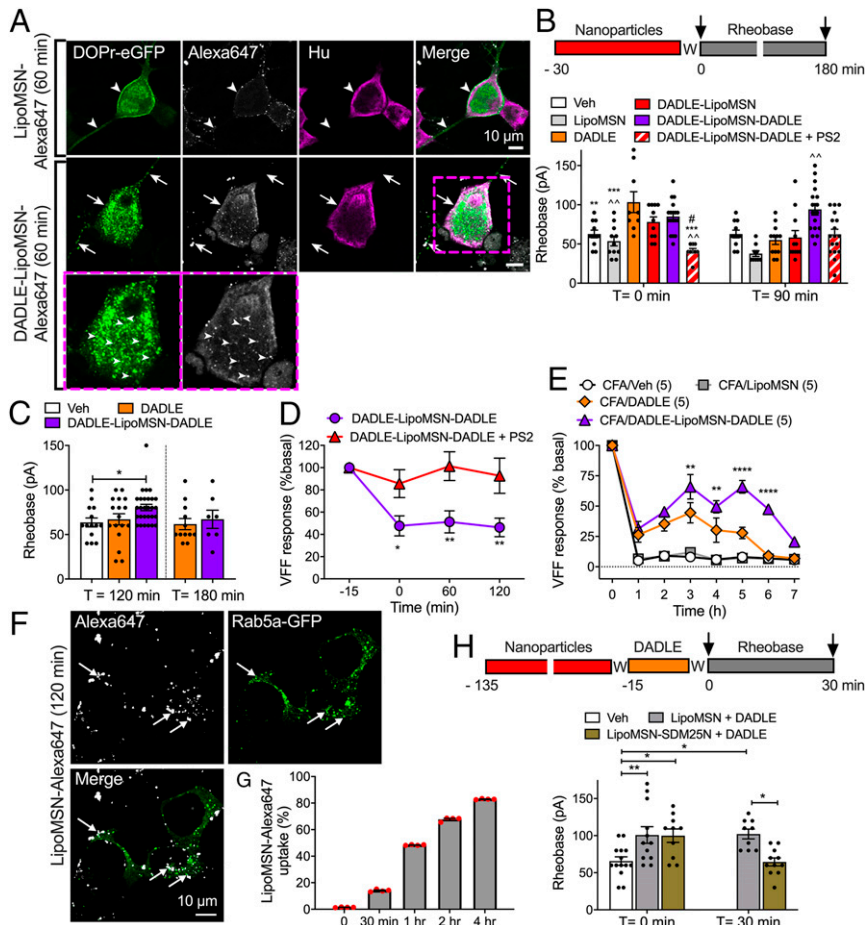
Fig. 8. Effects of nanoparticle-encapsulated DOPr ligands on nociceptors. (*A*) Uptake of LipoMSN-Alexa647 (control) or DADLE-LipoMSN-Alexa647 into primary cultures of DRG neurons from DOPr-eGFP mice. Neurons were incubated with nanoparticles for 60 min. Representative images from two experiments, from four mice. (*B* and *C*) Rheobase of mouse DRG neurons at 0, 90, 120, or 180 min after exposure to DADLE, DADLE-LipoMSN-DADLE, DADLE-LipoMSN (all 100 nM), LipoMSN (control), or vehicle (control) and washing. Some neurons were exposed to PS2 and DADLE-LipoMSN-DADLE. Data points indicate the number of studied neurons from $n = 6$ to 12 mice in *B* and *C* for each treatment. Compared with *DADLE, ^DADLE-LipoMSN-DADLE, and #DADLE-LipoMSN; *#$P < 0.05$, **^^$P < 0.01$, ***$P < 0.001$, one-way (*B*) or two-way (*C*) ANOVA with Tukey's post hoc test. (*D*) Colonic afferent activity at 0, 60, or 120 min after exposure of tissues to DADLE-LipoMSN-DADLE (100 nM). Some preparations were exposed to PS2 and DADLE-LipoMSN-DADLE. $n = 5$ mice per group. *$P < 0.05$, **$P < 0.01$, two-way (*) ANOVA with Sidak's post hoc test. (*E*) Ipsilateral paw withdrawal responses in mice. DADLE, DADLE-LipoMSN-DADLE (both 100 nM DADLE), LipoMSN, or vehicle (Veh) was injected intrathecally at 48 h after intraplantar CFA. $n = 5$ mice per group. **$P < 0.01$, ****$P < 0.0001$ DADLE compared with DADLE-LipoMSN-DADLE, two-way ANOVA with Tukey's multiple comparison post hoc test. (*F*) Uptake of LipoMSN-Alexa647 into endosomes of HEK293 cells expressing Rab5a-GFP after 120 min. (*G*) Time course of uptake of LipoMSN-Alexa647 into HEK293 cells. $n = 3$ independent experiments. (*H*) Rheobase of mouse DRG neurons. Neurons were incubated with LipoMSN-SDM25N (100 nM) or LipoMSN (control) for 120 min, washed (W), incubated with DADLE (10 nM, 15 min), and washed again. Rheobase was measured at 0 or 30 min after washing. Data points indicate the number of studied neurons from four mice for each treatment. *$P < 0.05$, **$P < 0.01$, two-way ANOVA with Tukey's post hoc test. All results are mean ± SEM.

permeability of the agonist (40). Although our results show that PKC and ERK mediate the inhibitory actions of endosomal DOPr on nociceptor excitability, the targets of these kinases and how they inhibit nociception remain to be defined. Toxicologic analysis of nanoparticle constituents, pharmacokinetic studies of nanoparticle cargo, and pharmacodynamic studies in preclinical models of pain will be necessary before this approach can be advanced to patients.

Materials and Methods

Animal Subjects. Institutional Ethics Committees approved the mouse studies.

Human Subjects. The Queen's University Human Ethics Committee approved the human studies. Patients undergoing colonoscopy for routine clinical care gave informed consent for biopsy specimens of the mucosa to be obtained from the descending colon during colonoscopy and for their data to be recorded for research purposes. Biopsy specimens of mucosa were collected from the descending colon of three patients with active cUC and three healthy control patients. Disease severity was evaluated using the endoscopy

component of the Mayo Clinic score for ulcerative colitis (*SI Appendix*, Table S1).

Colon Supernatants. Mice were treated for three cycles with 2% DSS in drinking water to induce chronic colitis or with water (control). Segments of whole colon were incubated in medium (24 h) to obtain supernatants (16–18). Biopsy specimens of colonic mucosa from cUC patients and controls (*SI Appendix*, Table S1) were incubated in medium to obtain supernatants (11, 52).

Patch Clamp Recording. Patch clamp recordings were made from mouse DRG neurons (11, 16, 18, 52). Neurons were preincubated for 60 min with supernatants and then washed. Neurons were stimulated for 15 min with DADLE (10 nM), SNC80 (10 nM), ARM390 (100 nM), DAMGO (10 nM), or vehicle (control) and then washed. Neurons were also incubated overnight (12 to 16 h) with DADLE (100 nM) or ARM390 (300 nM) and then washed. In some experiments, neurons were preincubated for 30 min with SDM25N (100 nM), CTOP (100 nM), Dy4 (30 µM), PS2 (15 µM), GF109203X (1 µM), PD98059 (50 µM), or vehicle. Rheobase was measured after agonist treatment and washing.

Extracellular Recording. Extracellular recordings were made from the lumbar splanchnic nerve innervating isolated mouse distal colon (11, 53, 54). SNC80, ARM390, or DAMGO (all 100 nM) was superfused into the organ bath for 15 min. In some studies, colon was preincubated for 15 min with PS2 (50 μM) before SNC80.

cDNAs, Cell Culture, and Transfection. Details are provided in *SI Appendix, Materials and Methods*.

Dissociation of DRG Neurons. DRG neurons were dispersed from DOPr-eGFP mice (55).

BRET Assays. BRET was measured in HEK293 cells (10, 26).

FRET Assays. FRET was measured in HEK293 cells and DRG neurons from DOPr-eGFP mice (10, 55). After FRET imaging, DOPr-eGFP was localized by immunofluorescence. FRET was measured in neurons expressing DOPr-eGFP.

DOPr-eGFP Trafficking. DRG neurons from DOPr-eGFP mice were exposed to vehicle, DADLE (1 μM), DADLE-LipoMSN-Alexa647 (1 μM DADLE), or LipoMSN-Alexa647 (10 μg/mL LipoMSN) (30 or 60 min, 37 °C). In some experiments, neurons were preincubated with Dy4 (30 μM) or PS2 (15 μM) (30 min). DOPr-eGFP in neurons was localized by immunofluorescence.

Preparation and Physicochemical Characterization of Nanoparticles. Details are provided in *SI Appendix, Materials and Methods*.

Cellular Targeting of LipoMSNs. HEK293-HA-DOPr or untransfected cells were incubated with DADLE-LipoMSN-Alexa647 or LipoMSN-Alexa647 (40 μg/mL). Uptake of nanoparticles was quantified by flow cytometry. In some experiments, cells were preincubated with Dy4, PS2, or inactive analogs (10 μg/mL, 30 min). For imaging studies, cells were transduced with Rab5a-GFP. After 24 h, cells were preincubated with rat anti-HA. Cells were washed and incubated with DADLE-LipoMSN-Alexa647 or LipoMSN-Alexa647 (20 μM DADLE, 200 μg/mL LipoMSN). HA-DOPr was localized by immunofluorescence. In some experiments, LipoMSN-Alexa647 uptake was examined by live cell imaging.

LipoMSNs and DOPr Signaling. Details are provided in *SI Appendix, Materials and Methods*.

LipoMSNs and Electrophysiology. Rheobase was measured at 0 to 180 min after exposure to DADLE or SDM25N nanoparticles and washing. Colonic afferent responses were assessed at 0 to 120 min after exposure to nanoparticles and washing.

LipoMSNs and Inflammatory Pain. The investigator was blinded to the treatments. Mice were assigned at random to treatments and acclimatized. CFA (0.5 mg/mL) was administered by intraplantar injection (10 μL) into the left hindpaw. DADLE (100 nM), DADLE-LipoMSN-DADLE (100 nM DADLE, 0.8 μg/mL LipoMSN), LipoMSN (1 μg/mL LipoMSN, control), or vehicle (control) was injected intrathecally (5 μL) at 48 h after CFA. Paw withdrawal to VFF was determined (10, 12).

1. A. S. Hauser, M. M. Attwood, M. Rask-Andersen, H. B. Schiöth, D. E. Gloriam, Trends in GPCR drug discovery: New agents, targets and indications. *Nat. Rev. Drug Discov.* **16**, 829–842 (2017).
2. K. E. Komolov, J. L. Benovic, G protein-coupled receptor kinases: Past, present and future. *Cell. Signal.* **41**, 17–24 (2018).
3. Y. K. Peterson, L. M. Luttrell, The diverse roles of arrestin scaffolds in G protein-coupled receptor signaling. *Pharmacol. Rev.* **69**, 256–297 (2017).
4. K. A. DeFea et al., The proliferative and antiapoptotic effects of substance P are facilitated by formation of a beta-arrestin-dependent scaffolding complex. *Proc. Natl. Acad. Sci. U.S.A.* **97**, 11086–11091 (2000).
5. K. A. DeFea et al., Beta-arrestin-dependent endocytosis of proteinase-activated receptor 2 is required for intracellular targeting of activated ERK1/2. *J. Cell Biol.* **148**, 1267–1281 (2000).
6. R. Irannejad, M. von Zastrow, GPCR signaling along the endocytic pathway. *Curr. Opin. Cell Biol.* **27**, 109–116 (2014).
7. J. E. Murphy, B. E. Padilla, B. Hasdemir, G. S. Cottrell, N. W. Bunnett, Endosomes: A legitimate platform for the signaling train. *Proc. Natl. Acad. Sci. U.S.A.* **106**, 17615–17622 (2009).
8. A. R. B. Thomsen, D. D. Jensen, G. A. Hicks, N. W. Bunnett, Therapeutic targeting of endosomal G protein-coupled receptors. *Trends Pharmacol. Sci.* **39**, 879–891 (2018).
9. P. Geppetti, N. A. Veldhuis, T. Lieu, N. W. Bunnett, G Protein-Coupled Receptors, G protein-coupled receptors: Dynamic machines for signaling pain and itch. *Neuron* **88**, 635–649 (2015).
10. D. D. Jensen et al., Neurokinin 1 receptor signaling in endosomes mediates sustained nociception and is a viable therapeutic target for prolonged pain relief. *Sci. Transl. Med.* **9**, eaal3447 (2017).
11. N. N. Jimenez-Vargas et al., Protease-activated receptor-2 in endosomes signals persistent pain of irritable bowel syndrome. *Proc. Natl. Acad. Sci. U.S.A.* **115**, E7438–E7447 (2018).
12. P. D. Ramírez-García et al., A pH-responsive nanoparticle targets the neurokinin 1 receptor in endosomes to prevent chronic pain. *Nat. Nanotechnol.* **14**, 1150–1159 (2019).
13. R. E. Yarwood et al., Endosomal signaling of the receptor for calcitonin gene-related peptide mediates pain transmission. *Proc. Natl. Acad. Sci. U.S.A.* **114**, 12309–12314 (2017).
14. G. Corder, D. C. Castro, M. R. Bruchas, G. Scherrer, Endogenous and exogenous opioids in pain. *Annu. Rev. Neurosci.* **41**, 453–473 (2018).
15. J. Boué et al., Endogenous regulation of visceral pain via production of opioids by colitogenic CD4(+) T cells in mice. *Gastroenterology* **146**, 166–175 (2014).
16. R. Guerrero-Alba et al., Co-expression of μ and δ opioid receptors by mouse colonic nociceptors. *Br. J. Pharmacol.* **175**, 2622–2634 (2018).
17. R. Guerrero-Alba et al., Stress activates pronociceptive endogenous opioid signalling in DRG neurons during chronic colitis. *Gut* **66**, 2121–2131 (2017).
18. E. Valdez-Morales et al., Release of endogenous opioids during a chronic IBD model suppresses the excitability of colonic DRG neurons. *Neurogastroenterol. Motil.* **25**, 39–46.e4 (2013).
19. M. Verma-Gandhu et al., CD4+ T-cell modulation of visceral nociception in mice. *Gastroenterology* **130**, 1721–1728 (2006).
20. G. Scherrer et al., Knockin mice expressing fluorescent delta-opioid receptors uncover G protein-coupled receptor dynamics in vivo. *Proc. Natl. Acad. Sci. U.S.A.* **103**, 9691–9696 (2006).
21. M. J. Robertson, F. M. Deane, P. J. Robinson, A. McCluskey, Synthesis of dynole 34-2, dynole 2-24 and dyngo 4a for investigating dynamin GTPase. *Nat. Protoc.* **9**, 851–870 (2014).
22. M. J. Robertson et al., Synthesis of the Pitstop family of clathrin inhibitors. *Nat. Protoc.* **9**, 1592–1606 (2014).
23. A. A. Pradhan et al., Agonist-specific recruitment of arrestin isoforms differentially modify delta opioid receptor function. *J. Neurosci.* **36**, 3541–3551 (2016).
24. D. Toullec et al., The bisindolylmaleimide GF 109203X is a potent and selective inhibitor of protein kinase C. *J. Biol. Chem.* **266**, 15771–15781 (1991).
25. D. T. Dudley, L. Pang, S. J. Decker, A. J. Bridges, A. R. Saltiel, A synthetic inhibitor of the mitogen-activated protein kinase cascade. *Proc. Natl. Acad. Sci. U.S.A.* **92**, 7686–7689 (1995).
26. D. D. Jensen et al., Endothelin-converting enzyme 1 and β-arrestins exert spatiotemporal control of substance P-induced inflammatory signals. *J. Biol. Chem.* **289**, 20283–20294 (2014).
27. A. A. Pradhan et al., In vivo delta opioid receptor internalization controls behavioral effects of agonists. *PLoS One* **4**, e5425 (2009).

28. D. P. Poole *et al.*, Localization and regulation of fluorescently labeled delta opioid receptor, expressed in enteric neurons of mice. *Gastroenterology* **141**, 982–991.e18 (2011).

29. Q. Wan *et al.*, Mini G protein probes for active G protein-coupled receptors (GPCRs) in live cells. *J. Biol. Chem.* **293**, 7466–7473 (2018).

30. R. Nehmé *et al.*, Mini-G proteins: Novel tools for studying GPCRs in their active conformation. *PLoS One* **12**, e0175642 (2017).

31. Y. Namkung *et al.*, Monitoring G protein-coupled receptor and β-arrestin trafficking in live cells using enhanced bystander BRET. *Nat. Commun.* **7**, 12178 (2016).

32. P. Donthamsetti, J. R. Quejada, J. A. Javitch, V. V. Gurevich, N. A. Lambert, Using bioluminescence resonance energy transfer (BRET) to characterize agonist-induced arrestin recruitment to modified and unmodified G protein-coupled receptors. *Curr. Protoc. Pharmacol.* **70**, 2 14 11–12 14 14 (2015).

33. M. L. Halls, M. Canals, Genetically encoded FRET biosensors to illuminate compartmentalised GPCR signalling. *Trends Pharmacol. Sci.* **39**, 148–157 (2018).

34. J. S. Herskovits, C. C. Burgess, R. A. Obar, R. B. Vallee, Effects of mutant rat dynamin on endocytosis. *J. Cell Biol.* **122**, 565–578 (1993).

35. C. Pinese *et al.*, Sustained delivery of siRNA/mesoporous silica nanoparticle complexes from nanofiber scaffolds for long-term gene silencing. *Acta Biomater.* **76**, 164–177 (2018).

36. D. Shao *et al.*, Bioinspired diselenide-bridged mesoporous silica nanoparticles for dual-responsive protein delivery. *Adv. Mater.*, e1801198 (2018).

37. J. J. DiCello *et al.*, Inflammation-associated changes in DOR expression and function in the mouse colon. *Am. J. Physiol. Gastrointest. Liver Physiol.* **315**, G544–G559 (2018).

38. C. M. Cahill, S. V. Holdridge, A. Morinville, Trafficking of delta-opioid receptors and other G-protein-coupled receptors: Implications for pain and analgesia. *Trends Pharmacol. Sci.* **28**, 23–31 (2007).

39. A. A. Pradhan *et al.*, Ligand-directed trafficking of the δ-opioid receptor in vivo: Two paths toward analgesic tolerance. *J. Neurosci.* **30**, 16459–16468 (2010).

40. M. Stoeber *et al.*, A genetically encoded biosensor reveals location bias of opioid drug action. *Neuron* **98**, 963–976.e5 (2018).

41. M. Narita, H. Mizoguchi, J. P. Kampine, L. F. Tseng, Role of protein kinase C in desensitization of spinal delta-opioid-mediated antinociception in the mouse. *Br. J. Pharmacol.* **118**, 1829–1835 (1996).

42. E. G. Ignatova, M. M. Belcheva, L. M. Bohn, M. C. Neuman, C. J. Coscia, Requirement of receptor internalization for opioid stimulation of mitogen-activated protein kinase: Biochemical and immunofluorescence confocal microscopic evidence. *J. Neurosci.* **19**, 56–63 (1999).

43. W. H. De Jong, P. J. Borm, Drug delivery and nanoparticles: Applications and hazards. *Int. J. Nanomedicine* **3**, 133–149 (2008).

44. O. C. Farokhzad, R. Langer, Impact of nanotechnology on drug delivery. *ACS Nano* **3**, 16–20 (2009).

45. K. E. Uhrich, S. M. Cannizzaro, R. S. Langer, K. M. Shakesheff, Polymeric systems for controlled drug release. *Chem. Rev.* **99**, 3181–3198 (1999).

46. H. Maeda, J. Wu, T. Sawa, Y. Matsumura, K. Hori, Tumor vascular permeability and the EPR effect in macromolecular therapeutics: A review. *J. Control. Release* **65**, 271–284 (2000).

47. G. K. Such, Y. Yan, A. P. Johnston, S. T. Gunawan, F. Caruso, Interfacing materials science and biology for drug carrier design. *Adv. Mater.* **27**, 2278–2297 (2015).

48. C. E. Nelson *et al.*, Balancing cationic and hydrophobic content of PEGylated siRNA polyplexes enhances endosome escape, stability, blood circulation time, and bioactivity in vivo. *ACS Nano* **7**, 8870–8880 (2013).

49. D. Calebiro *et al.*, Persistent cAMP-signals triggered by internalized G-protein-coupled receptors. *PLoS Biol.* **7**, e1000172 (2009).

50. R. Irannejad *et al.*, Conformational biosensors reveal GPCR signalling from endosomes. *Nature* **495**, 534–538 (2013).

51. R. J. Park *et al.*, Dynamin triple knockout cells reveal off target effects of commonly used dynamin inhibitors. *J. Cell Sci.* **126**, 5305–5312 (2013).

52. E. E. Valdez-Morales *et al.*, Sensitization of peripheral sensory nerves by mediators from colonic biopsies of diarrhea-predominant irritable bowel syndrome patients: A role for PAR2. *Am. J. Gastroenterol.* **108**, 1634–1643 (2013).

53. S. M. Brierley, R. C. Jones, 3rd, G. F. Gebhart, L. A. Blackshaw, Splanchnic and pelvic mechanosensory afferents signal different qualities of colonic stimuli in mice. *Gastroenterology* **127**, 166–178 (2004).

54. P. A. Hughes *et al.*, Post-inflammatory colonic afferent sensitisation: Different subtypes, different pathways and different time courses. *Gut* **58**, 1333–1341 (2009).

55. M. L. Halls, D. P. Poole, A. M. Ellisdon, C. J. Nowell, M. Canals, Detection and quantification of intracellular signaling using FRET-based biosensors and high content imaging. *Methods Mol. Biol.* **1335**, 131–161 (2015).